A dual-circuit causal model of depression in humans

Summer Frandsen
Brigham & Women's Hospital, Brandeis University https://orcid.org/0000-0003-0306-3018
Cory Glover
Northeastern University
Robin Cash
University of Melbourne
Daniel Blumberger
Centre for Addiction and Mental Health https://orcid.org/0000-0002-8422-5818
Ki Sueng Choi
Icahn School of Medicine at Mount Sinai https://orcid.org/0000-0002-6446-0677
Darin Dougherty
Massachusetts General Hospital https://orcid.org/0000-0003-4691-4353
Jonathan Downar
Centre for Addiction and Mental Health, University of Toronto
Paul Fitzgerald
Epworth Healthcare, Monash University
Mark George
Medical University of South Carolina
Andreas Horn
Brigham & Women's Hospital https://orcid.org/0000-0002-0695-6025
Friederike Grospietsch
Charite University Medicine Berlin
Kevin Johnson
Florida State University
Andrea Kühn
Charité - Universitätsmedizin Berlin https://orcid.org/0000-0002-4134-9060
Helen Mayberg
Icahn School of Medicine at Mount Sinai https://orcid.org/0000-0002-1672-2716
Alvaro Pascual-Leone
Harvard Medical Medical School https://orcid.org/0000-0001-8975-0382
Patricio Riva-Posse
Emory University
Rob Rouhl

Maastricht University Medical Center

Frederic Schaper

Center of Brain Circuit Therapeutics, Departments of Neurology, Psychiatry, and Radiology, Brigham and Women's Hospital https://orcid.org/0000-0001-5487-0923

Stephan Taylor

University of Michigan School of Medicine

Yasin Temel

Maastricht University Medical Center

Fidel Vila-Rodriguez

University of British Columbia https://orcid.org/0000-0002-8273-8820

Andrew Zalesky

Melbourne Neuropsychiatry Centre, University of Melbourne, Melbourne, Australia; Department of Biomedical Engineering, University of Melbourne, Melbourne, Australia.

Jordan Grafman

Shirley Ryan AbilityLab https://orcid.org/0000-0001-8645-4457

Shan Siddiqi

shsiddiqi@bwh.harvard.edu

Harvard Medical School, Brigham & Women's Hospital https://orcid.org/0000-0002-0967-9289

Biological Sciences - Article

Keywords:

Posted Date: February 2nd, 2024

DOI: https://doi.org/10.21203/rs.3.rs-3754811/v1

Additional Declarations: Yes there is potential Competing Interest. SHS serves as a consultant for Kaizen Brain Center, Acacia Mental Health, and Magnus Medical. SHS owns stock in Brainsway Ltd (publicly traded) and Magnus Medical (not publicly traded). SHS has received investigator-initiated research support from Neuronetics Inc and Brainsway Ltd. SHS owns independent intellectual property on the use of brain network mapping to target neuromodulation. DMB has received research support from Brain Canada, CIHR, NIH, and the Temerty Family Foundation through the CAMH Foundation and Campbell Institute. DMB has received research support and in-kind equipment support and was the site principal investigator for sponsor-initiated studies from BrainsWay. DMB has received in-kind equipment support from MagVenture for investigator-initiated studies, medication supplies for an investigator-initiated trial

from Indivior, and has served on advisory boards for Janssen and Welcony. KSC receives consulting fees from Abbott Neuromodulation. DDD's research has been funded by the International OCD Foundation, Brain and Behavior Research Foundation, National Institute of Mental Health, Tiny Blue Dot Foundation and Medtronic. DDD has received honoraria and consultation fees from Medtronic, Sage, and Celanese and has equity in Neurable, Innercosmos, and Intrinsic Powers. JD has received research support from the Arrell Family Foundation, Brain Canada, the Buchan Family Foundation, the Canadian Biomarker Integration Network in Depression, CIHR, the Klarman Family Foundation, NIH, the Ontario Brain Institute, the Toronto General and Western Hospital Foundation, and the Weston Family Foundation. JD has received travel stipends from ANT Neuro and Lundbeck. JD has served as an adviser for BrainCheck, Restorative Brain Clinics, and TMS Neuro Solutions, and has equity ownership in Neurostim TMS Centers, Restorative Brain Clinics, and Salience Neuro Health. PBF has received equipment for research from Neurosoft, Nexstim and Brainsway Ltd. PBF has served on scientific advisory boards for Magstim and LivaNova and received speaker fees from Otsuka. PBF has also acted as a founder and board member for TMS Clinics Australia and Resonance Therapeutics. MSG has filed a record of invention for using EEG phase synchronized TMS for treatment of brain diseases. No patents have been issued yet. MSG acts as a paid consultant for Abbott (Boston Scientific), Sooma, Neurolief and an unpaid consultant for Brainsway, Magnus medical. MSG also has research grants to MUSC from Livanova and Magnus Medical. AH reported personal fees from Boston Scientific. KAJ received grant support from the Department of Defense—unrelated medical device consulting (ACI, LLC.). AAK is supported by the Deutsche Forschungsgemeinschaft (DFG, German Research Foundation) Project-ID 424778381 TRR 295 and under Germany's Excellence Strategy EXC-2049 390688087 (Project Neurocure-BrainLab) and is supported by the Lundbeck Foundation as part of the collaborative project grant "Adaptive and precise targeting of cortex-basal ganglia circuits in Parkinson's disease" (R336-2020-1035). AAK has served on advisory boards of Medtronic and has received honoraria and travel support from Medtronic, Boston Scientific, Ipsen Pharma, and Teva. HSM receives consulting and IP licensing fees from Abbott labs and is listed as an inventor on provisional patent filings. AP-L is a co-founder of TI Solutions AG, a company committed to producing hardware and software solutions to support TI research. A.P.-L. is inventor on several issued and pending patents on the real-time integration of non-invasive brain stimulation with electroencephalography and MRI, and applications of non-invasive brain stimulation in various neurological disorders, as well as digital biomarkers of cognition and digital assessments for early diagnosis of dementia. PR-P receives consulting fees from Abbott Neuromodulation, LivaNova, and Janssen Pharmaceuticals. FLWVJS reported grants from the American Epilepsy Society, the National Institute of Neurological Disorders and Stroke, the Royal Netherlands Academy of Arts and Sciences, the Dr Jan Meerwaldt Stichting, and Stichting De Drie Lichten during the conduct of the study. FV-R has received research support from Brain Canada, CIHR, the Michael Smith Foundation for Health Research, the Vancouver Coastal Health Research Institute, and the Weston Brain Institute for investigator-initiated research; 238 ajp.psychiatryonline.org Am J Psychiatry 180:3, March 2023 FUNCTIONAL CONNECTIVITY MAPPING FOR rTMS TARGET SELECTION IN DEPRESSION. FV-R has received philanthropic support from the Seedlings Foundation, in-kind equipment support for this investigator-initiated trial from MagVenture, and honoraria for participation on an advisory board for Janssen. AZ reported grants from National

Health and Medical Research Council Senior Research Fellowship. None of the described organizations or intellectual property were involved in the present work. All other authors have no competing interests to disclose.

Abstract

Therapeutic brain stimulation targets are typically designed to treat specific psychiatric or neurological symptoms.[1–4] This approach presents a dilemma when treating patients with comorbidities, atypical symptom profiles, or overlapping symptoms. Identifying targets that modulate groups of behavioral or cognitive symptoms across diagnoses may provide alternative treatment options and outcomes. Here, we use causal brain mapping and clustering methods to identify two distinct brain networks, based on common patterns of connectivity to lesions that selectively modify behaviors and symptoms. Due to the behavioral items in each cluster, we hypothesize that these networks are related to positive and negative affect, respectively. Across ten different datasets of patients receiving transcranial magnetic stimulation (TMS) or deep brain stimulation (DBS),[1,5,6] stimulation site connectivity to each of our two brain networks independently predicted improvement in depressive symptoms. Thus, we defined two networks which are independently and causally involved in depression symptoms.

Introduction

Therapeutic neuromodulation for psychiatric disorders is largely based on targeting a single circuit for a single symptom or disorder.[1–4] This model is incomplete in at least two ways. First, a disorder may be associated with various symptom profiles that map to heterogeneous circuits, yielding distinct “biotypes” that respond to different treatments.[7–10] Second, a disorder may have overlapping symptoms such as absence of positive affect versus presence of negative affect, which map to different circuitry in animal models but are difficult to distinguish in humans.[11–13]

These challenges may be partly addressed by finding brain stimulation sites that target distinct brain circuits associated with distinct clusters behaviors.[9,14,15] Our group has previously validated methods to cluster symptoms based on the connectivity of transcranial magnetic stimulation (TMS) sites that causally modify those symptoms.[9] However, these methods were limited to detecting symptoms that were measured by conventional clinical scales and were selectively modified by different TMS sites within the dorsolateral prefrontal cortex (DLPFC). Additional circuit-based behavioral clusters may exist, but would be best detected using a method that provides whole-brain coverage along with deep phenotyping.

This may be achieved using brain lesion data. Because incidental lesions can occur in widely different brain regions, they can be used to study the causal effects of damage to different brain circuits.[16] Our group recently demonstrated that brain lesions causing depression are connected to the same circuit as TMS sites and deep brain stimulation (DBS) sites that modify depression, suggesting that lesion-derived circuits may be relevant to targeting brain stimulation.[6,16] Similar results have since been observed for motor and cognitive symptoms of Parkinson’s disease, epilepsy, tremor, addiction, and tics.[6,17–21] Thus, if specific clusters of behaviors are modified by damage to distinct brain circuits, the same circuits would be promising candidates for therapeutic TMS and DBS targets.[22] If successful, this would not only

optimize brain stimulation for depression, but would also illustrate a new approach for classifying behaviors based on causal neuroanatomy and deriving new therapeutic targets.

Here, we apply causal human brain mapping methods to identify two distinct clusters of behaviors that map to two distinct brain circuits. Stimulation site connectivity to these two distinct circuits independently predicted clinical antidepressant outcomes after TMS and DBS, demonstrating that both circuits play an independent causal role in symptoms of depression.

Results

Clustering two distinct circuits

First, in 196 military Veterans who suffered penetrating head trauma during the Vietnam

War, we mapped the circuitry of brain lesions that modified 185 different behavioral metrics (listed in Table S1). These “behaviors” included neuropsychiatric symptoms, diagnoses, traits, and other self-report measures collected during an extensive phenotyping battery.[23,24] For each measure, a higher score indicates more of the associated behavior (e.g. higher score on BDI sadness item means higher levels of sadness). As in our prior work,[25,26] we localized each lesion on a standard MNI brain template (Fig. 1a) and estimated its whole-brain resting-state functional connectivity (rsFC) profile (Fig. 1b) using a normative connectome database (n=1000).[27] Across all participants, lesion connectivity to each voxel was compared with each behavioral measure using Pearson correlations, yielding 185 behavioral circuit maps (Fig. 1c).

Next, we tested whether these 185 circuits were significantly different from each other.

We computed the pairwise spatial correlation between all possible pairs of behavioral circuits (Fig. 2a), and quantified the overall heterogeneity in these 185 circuits based on the variance in these spatial correlations (SD=.48). This heterogeneity was significantly stronger than chance as determined by permutation testing (p=.02) (Fig. 2b) in which the variance was recomputed 25,000 times after randomly shuffling each patient’s clinical outcomes with a different patient’s neuroimaging results, as in our prior work.[6] A p-value was computed as the percentage of cases in which the permuted value was greater than the real variance.

We then classified the 185 circuit maps using Ward’s hierarchical clustering algorithm.[28]

The optimal number of clusters was 2 (silhouette coefficient=.68, p=.04, 25,000 permutations) (Fig. 2c). We also compared the top three cluster solutions (k=2, 3, 4) using additional community detection algorithms per standards of best practice[29], yielding similar results (Figure S1). We also observed similar results after repeating the analysis with different data cleaning approaches (Table S2).

Cluster quality analyses

As a control analysis, we tested whether similar clustering could be achieved based on cross-correlations in behavioral data alone, without incorporating anatomical data. No clear clusters were apparent when using behavioral data alone (Fig. 2d).

To show that the clusters were not driven by any one behavior, we performed a leaveone-behavior-out analysis by computing the spatial correlation of each map to the mean of the remaining behavioral maps in the same cluster. These leave-one-out spatial correlation values were significantly stronger than zero for both clusters (one-sample t-test $p<10^{-16}$). To account for outliers, we removed any behavioral circuit maps that were negatively correlated with their own cluster, and repeated the leave-one-behavior-out analysis with the cleaned dataset. Four of the 185 behaviors were excluded as outliers. We repeated this process in a second iteration, and no additional outliers were detected.

We used these re-computed spatial correlation values to determine the most central and representative behaviors in each cluster. The top 5 central maps of Cluster 1 (58 items) were “depressive disorder not otherwise specified”, “carefree”, “opioid abuse,” “vigorous,” and

“friendly” while the top 5 maps of Cluster 2 (124 items) were “guilt”, “anger”, “paranoia,” “helpless,” and “sadness”. See Tables S3-5 and Figure S2 for a full list of rankings before and after data cleaning.

Final whole-brain cluster maps

We then generated an overall circuit map for both clusters by averaging their respective individual behavior circuit maps (Fig. 3a). These final two cluster maps show the connectivity of lesions that modify the behaviors within each cluster. We identified the locations of significant voxels (Fig. 3b) in each cluster map using the Westfall-Young method as implemented by Winkler et al.[30] Cluster 1 had peaks in the posterior cingulate cortex (PCC), in the tapetum of the corpus callosum in a region that connects the two medial temporal lobes to each other,[31] and in the ventral midbrain, including the ventral tegmental area (VTA) and substantia nigra (SN) (max

$|r|=0.13$, $p_{FWE}=0.02$). Cluster 2 had a peak in the pituitary gland (max $|r|=0.16$, $p_{FWE}=0.03$) (Fig. 3c, Figure S3). Because peak-voxel values may be misleading when analyzing the overall topography of a broader circuit, we repeated the analysis using the absolute mean voxel value (Cluster 1: mean $|r|=.06$, $p<.001$; Cluster 2: mean $|r|=.06$, $p=0.01$). See Table S6 for data variations.

Predicting clinical outcomes

To assess the clinical utility and causal relevance of our two circuits, we used them to predict TMS and DBS antidepressant outcomes (Fig. 4). We hypothesized that stimulation site connectivity to each of the two circuits would independently predict treatment-induced change in depression. These analyses utilized 10 independent, previously published datasets[1,5,6] which included stimulation sites and depression scores before and after treatment for 554 patients. In five DBS datasets (total n=101) and four TMS datasets (total n=151), patients were stimulated at various sites due to incidental variability in routine

clinical targeting procedures, and connectivity of these sites was estimated following our published methods on deriving a convergent depression circuit.[6] In one TMS dataset (total n=302), all participants were stimulated at the same MNI coordinate, and completed a baseline resting-state fMRI scan, enabling analysis of the individualized differences between patients' TMS site connectivity values.[1,5]

To estimate the connectivity of patients' stimulation sites to our two circuits, we computed the spatial correlation of each cluster circuit (Fig. 4a) with each stimulation site's connectivity profile (Fig. 4b). For each cluster, we used these connectivity values to predict treatment-induced change in depression (Fig. 4c) using partial Pearson correlations, controlling for the effect of connectivity to the other cluster and baseline depression scores. Each dataset was analyzed individually and then combined using a weighted mean (Fig. 4d). The significance of these findings was confirmed via permutation testing. Treatment-induced change in depression was independently predicted by stimulation site connectivity to Cluster 1 (partial r=.18, p<.001) and Cluster 2 (partial r=.13, p=.002). This was independently true for the combined nine normative connectivity datasets with variable stimulation sites (n=252, Cluster 1: r=.24, p<.001, Cluster 2: r=.15, p=.02), and for the individualized connectivity dataset with consistent stimulation sites (n=302, Cluster 1: r=.13, p=.01, Cluster 2: r=.11, p=.008). See Table S8 for individual dataset prediction

Discussion

Clustering symptoms has become an increasingly common approach to precision medicine in fields ranging from oncology to psychiatry.[34–36] Recent work has laid the groundwork for clustering symptoms using behavioral-anatomical data.[9] While previous approaches used TMS data from patients with major depression, we applied similar methods to a lesion dataset with deep phenotyping across multiple psychiatric disorders, as lesions that modify a symptom have been shown to overlap with the same circuit as TMS and DBS sites that modify

the same symptom.[6,17–21] This approach enables derivation of overall symptom cluster circuit maps which can be used to inform therapeutic development, including identifying neuromodulation targets.

We first confirmed the existence of at least two distinct anatomical circuits associated with different clusters of behaviors, symptoms, and traits. Based on the primary behaviors in each cluster, we propose a two-circuit model of affect in which Cluster 1 is associated with positive affect (e.g. "carefree," "vigorous," and "opiate abuse") and Cluster 2 is associated with negative affect (e.g. "guilt", "helpless," "sadness"). Of note, unspecified depression was one of the top maps in the positive affect cluster. This diagnosis is given only to patients who do not meet criteria for major depressive disorder (MDD), such as those in whom substance abuse may be a complicating factor. Thus, the two-cluster model may help distinguish between different diagnoses that share similar symptoms.

Cluster 1 included three peak locations that survived multiple comparisons correction: the VTA/SN, the PCC, and the tapetum of the corpus callosum. As the sources of dopamine in the mesolimbic reward system and the nigrostriatal tract, the VTA and SN have long been implicated in the regulation of positive

affect in both animal models and human studies.[37–41] This is consistent with our finding that lesions negatively connected to these areas were associated with positive affect. Functional abnormalities in the PCC have also been implicated in blunted positive affect.[42] The tapetum of the corpus callosum is a white matter region that connects the two hippocampi to each other, and thus may be an epiphenomenon that arises due to independent involvement of both medial temporal lobes.[31]

Cluster 2 had a peak in the pituitary gland, potentially suggesting involvement of the hypothalamic-pituitary-adrenal (HPA) axis, which secretes cortisol throughout the body. This is consistent with studies implicating cortisol in states of chronic stress, negative affect, and MDD.[43–46] However, the pituitary itself is typically excluded from whole-brain functional connectivity analyses, so it may be systematically understudied in the neuroimaging literature. Nevertheless, our findings may bring together two established models of affect – the neurotransmitter model involving dopamine and the hormone model involving cortisol.

Perhaps most importantly, our lesion-derived behavioral clusters predicted outcomes with therapeutic brain stimulation. Stimulation site connectivity to each cluster independently predicted antidepressant response across ten brain stimulation studies. This builds on our prior work suggesting that brain stimulation treatments for depression can be optimized by targeting a specific "depression circuit."[6] While the idea of circuit-based targeting may still be true in principle, the present results suggest that efficacy may be further optimized by choosing a stimulation site that is connected to both the positive and negative affect circuits, not just a single depression circuit. This is consistent with recent work demonstrating that antidepressant efficacy of DBS can be optimized by targeting the intersection of multiple fiber tracts rather than a single

circuit.[47,48]

At present, this dual-circuit approach may be used to refine treatment sites within the standard treatment protocol (e.g. TMS to the dorsolateral prefrontal cortex for MDD). However, further research is needed to incorporate other factors such as modality. For example, although our collective predictive stimulation dataset has 101 DBS patients, our TMS sample was substantially larger. Future studies should investigate if there is a difference in the most effective way to target both circuits based on modality of treatment, or if one circuit is more suitable for a specific treatment type. Similarly, different brain regions may react differently to brain stimulation due to differences in features like cortical excitability or synaptic plasticity. Larger and more deeply phenotyped brain stimulation datasets could help identify the ideal entry point to access the circuit. Based on these factors, patients may need to be stratified to one target or the other, rather than targeting both circuits.

While we demonstrated the existence and therapeutic relevance of two distinct behavioral clusters, our results and methods were based on imprecise and heterogeneous data, which introduces noise and likely limits our measured effect size. For instance, since there were no preinjury baseline scores, our methods assume that pre-lesion scores were randomly distributed with respect to lesion location. Additionally, the

behaviors included in the analysis incorporated a wide variety of items, many of which are likely unrelated to one another (e.g. validity, affective, and cognitive scales). Our results are also limited by the possible mis-classification of some individual items within each cluster, particularly those near the overlap of the two clusters.[49] This is an inherent limitation to clustering analyses, and a perfect classification would suggest an overfit and ungeneralizable model.[49,50] Our methods were designed to demonstrate the existence of two clusters, but are not able to establish the constituents of each cluster with certainty. In addition, we applied the clustering algorithm to whole-brain correlations which distill the circuit to single metrics. The strength of our final cluster maps is similarly limited by averaging across every individual behavior map, increasing the difficulty of identifying peaks. Finally, our analyses were retrospective based on natural experiments that were readily available. Datasets were heterogeneous in many ways including population, treatment site, outcome measures, etc. More precise effect sizes may be expected with prospective studies that include deep phenotyping and stimulation of different targets. Future studies could address these sources of noise with dedicated affective phenotyping before and after brain stimulation, which may reveal additional clusters or additional anatomical associations.

Finally, it should be noted that we tested depression outcomes based on data availability. But, due to our deeply phenotyped approach, our clusters are broad in scope and could be considered potentially transdiagnostic in nature. Thus, future studies should evaluate these targets in context of other disorders with affective components, such as addiction, chronic pain, or personality disorders.

Overall, we identified two distinct circuits connected to lesions potentially associated with positive and negative affect. Both circuits were derived from causal lesions, and were validated against causal TMS and DBS sites. Stimulation site connectivity to each of these circuits independently predicted improvement in depression, indicating that both are independently and causally involved in depression. This dual-circuit model may also be applicable across various disorders, creating a common circuit and treatment target for affective symptoms.

Declarations

Acknowledgements

This material is based upon work supported by the National Science Foundation Graduate Research Fellowship Program under Grant No. 2139752. Any opinions, findings, and conclusions or recommendations expressed in this material are those of the authors and do not necessarily reflect the views of the National Science Foundation. The authors would also like to thank the National Institute of Mental Health and Baszucki Family Foundation for funding this work.

Competing Interests

SHS serves as a consultant for Kaizen Brain Center, Acacia Mental Health, and Magnus Medical. SHS owns stock in Brainsway Ltd (publicly traded) and Magnus Medical (not publicly traded). SHS has received investigator-initiated research support from Neuronetics Inc and Brainsway Ltd. SHS owns

independent intellectual property on the use of brain network mapping to target neuromodulation. DMB has received research support from Brain Canada, CIHR, NIH, and the Temerty Family Foundation through the CAMH Foundation and Campbell Institute. DMB has received research support and in-kind equipment support and was the site principal investigator for sponsor-initiated studies from BrainsWay. DMB has received in-kind equipment support from MagVenture for investigator-initiated studies, medication supplies for an investigator-initiated trial from Indivior, and has served on advisory boards for Janssen and Welcony. KSC receives consulting fees from Abbott Neuromodulation. DDD's research has been funded by the International OCD Foundation, Brain and Behavior Research Foundation, National Institute of Mental Health, Tiny Blue Dot Foundation and Medtronic. DDD has received honoraria and consultation fees from Medtronic, Sage, and Celanese and has equity in Neurable, Innercosmos, and Intrinsic Powers. JD has received research support from the Arrell Family Foundation, Brain Canada, the Buchan Family Foundation, the Canadian Biomarker Integration Network in Depression, CIHR, the Klarman Family Foundation, NIH, the Ontario Brain Institute, the Toronto General and Western Hospital Foundation, and the Weston Family Foundation. JD has received travel stipends from ANT Neuro and Lundbeck. JD has served as an adviser for BrainCheck, Restorative Brain Clinics, and TMS Neuro Solutions, and has equity ownership in Neurostim TMS Centers, Restorative Brain Clinics, and Salience Neuro Health. PBF has received equipment for research from Neurosoft, Nexstim and Brainsway Ltd. PBF has served on scientific advisory boards for Magstim and LivaNova and received speaker fees from Otsuka. PBF has also acted as a founder and board member for TMS Clinics Australia and Resonance Therapeutics. MSG has filed a record of invention for using EEG phase synchronized TMS for treatment of brain diseases. No patents have been issued yet. MSG acts as a paid consultant for Abbott (Boston Scientific), Sooma, Neurolief and an unpaid consultant for Brainsway, Magnus medical. MSG also has research grants to MUSC from Livanova and Magnus Medical. AH reported personal fees from Boston Scientific. KAJ received grant support from the Department of Defense—unrelated medical device consulting (ACI, LLC.). AAK is supported by the Deutsche Forschungsgemeinschaft (DFG, German Research Foundation) Project-ID 424778381 TRR 295 and under Germany's Excellence Strategy EXC-2049 390688087 (Project Neurocure-BrainLab) and is supported by the Lundbeck Foundation as part of the collaborative project grant "Adaptive and precise targeting of cortex-basal ganglia circuits in Parkinson's disease" (R336-2020-1035). AAK has served on advisory boards of Medtronic and has received honoraria and travel support from Medtronic, Boston Scientific, Ipsen Pharma, and Teva. HSM receives consulting and IP licensing fees from Abbott labs and is listed as an inventor on provisional patent filings. AP-L is a co-founder of TI Solutions AG, a company committed to producing hardware and software solutions to support TI research. A.P.-L. is inventor on several issued and pending patents on the real-time integration of non-invasive brain stimulation with electroencephalography and MRI, and applications of non-invasive brain stimulation in various neurological disorders, as well as digital biomarkers of cognition and digital assessments for early diagnosis of dementia. PR-P receives consulting fees from Abbott Neuromodulation, LivaNova, and Janssen Pharmaceuticals. FLWVJS reported grants from the American Epilepsy Society, the National Institute of Neurological Disorders and Stroke, the Royal Netherlands Academy of Arts and Sciences, the Dr Jan Meerwaldt Stichting, and Stichting De Drie Lichten during the conduct of the study. FV-R has received research support from Brain Canada, CIHR, the Michael Smith

Foundation for Health Research, the Vancouver Coastal Health Research Institute, and the Weston Brain Institute for investigator-initiated research; 238 ajp.psychiatryonline.org Am J Psychiatry 180:3, March 2023 FUNCTIONAL CONNECTIVITY MAPPING FOR rTMS TARGET SELECTION IN DEPRESSION. FV-R has received

philanthropic support from the Seedlings Foundation, in-kind equipment support for this investigator-initiated trial from MagVenture, and honoraria for participation on an advisory board for Janssen. AZ reported grants from National Health and Medical Research Council Senior Research Fellowship. None of the described organizations or intellectual property were involved in the present work. All other authors have no competing interests to disclose.

Data Availability

This paper used de-identified data from 11 different datasets collected by 11 different teams of investigators at various institutions across different countries. Each dataset is available upon reasonable request from each respective team of investigators. Data sharing will be subject to the policies and procedures of the institution where each dataset was collected as well as the laws of the country where each dataset was collected.

Code Availability

Personalized MATLAB and python scripts used for preprocessing and analyses can be found at https://siddiqi.bwh.harvard.edu/data-code/and https://github.com/alexlicohen. Additional code available upon reasonable request.

Author Contributions

SBF conducted all analyses. CG assisted with analyses and figure design. RFHC assisted with additional validation analyses. JHG collected and provided the VHIS dataset. DMB, RFHC,

KSC, DDD, JD, PBF, MSG, AH, FI, KAJ, AK, HSM, APL, PRP, RPWR, FLWVJS, SFT, YT,

FVR, and AZ collected and provided the ten clinical validation datasets. SHS supervised all analyses. SBF and SHS wrote the manuscript with input from all authors.

References

1. Blumberger, D. M. *et al.* Effectiveness of theta burst versus high-frequency repetitive transcranial magnetic stimulation in patients with depression (THREE-D): a randomised non-inferiority trial. *The Lancet***391**, 1683–1692 (2018).
2. Fox, M. D., Buckner, R. L., White, M. P., Greicius, M. D. & Pascual-Leone, A. Efficacy of TMS targets for depression is related to intrinsic functional connectivity with the subgenual cingulate. *Biol. Psychiatry***72**, 595–603 (2012).

3. Gomes, P. V. O., Brasil-Neto, J. P., Allam, N. & Rodrigues de Souza, E. A Randomized, Double-Blind Trial of Repetitive Transcranial Magnetic Stimulation in Obsessive-Compulsive Disorder With Three-Month Follow-Up. *J. Neuropsychiatry Clin. Neurosci.***24**, 437–443 (2012).
4. Williams, N. R. *et al.* Accelerated neuromodulation therapy for Obsessive-Compulsive Disorder. *Brain Stimul. Basic Transl. Clin. Res. Neuromodulation***14**, 435–437 (2021).
5. Elbau, I. G. *et al.* Functional Connectivity Mapping for rTMS Target Selection in Depression. *Am. J. Psychiatry***180**, 230–240 (2023).
6. Siddiqi, S. H. *et al.* Brain stimulation and brain lesions converge on common causal circuits in neuropsychiatric disease. *Nat. Hum. Behav.***5**, 1707–1716 (2021).
7. Drysdale, A. T. *et al.* Resting-state connectivity biomarkers define neurophysiological subtypes of depression. *Nat. Med.***23**, 28–38 (2017).
8. Goldstein-Piekarski, A. N. *et al.* Mapping Neural Circuit Biotypes to Symptoms and Behavioral Dimensions of Depression and Anxiety. *Biol. Psychiatry***91**, 561–571 (2022).
9. Siddiqi, S. H. *et al.* Distinct Symptom-Specific Treatment Targets for Circuit-Based Neuromodulation. *Am. J. Psychiatry* (2020) doi:10.1176/appi.ajp.2019.19090915.
10. Williams, L. M. Defining biotypes for depression and anxiety based on large-scale circuit dysfunction: A theoretical review of the evidence and future directions for clinical translation. *Depress. Anxiety***34**, 9–24 (2017).
11. Forbes, E. E. & Dahl, R. E. Neural Systems of Positive Affect: Relevance to Understanding Child and Adolescent Depression? *Dev. Psychopathol.***17**, 827–850 (2005).
12. Namburi, P. *et al.* A circuit mechanism for differentiating positive and negative associations. *Nature***520**, 675–678 (2015).
13. Ye, L. *et al.* Wiring and Molecular Features of Prefrontal Ensembles Representing Distinct Experiences. *Cell***165**, 1776–1788 (2016).
14. Workman, C. D., Kamholz, J. & Rudroff, T. Transcranial direct current stimulation (tDCS) for the treatment of a Multiple Sclerosis symptom cluster. *Brain Stimulat.***13**, 263–264 (2020).
15. Zhao, Y. *et al.* Anterior Cingulate Cortex in Addiction: New Insights for Neuromodulation. *Neuromodulation Technol. Neural Interface***24**, 187–196 (2021).
16. Siddiqi, S. H., Kording, K. P., Parvizi, J. & Fox, M. D. Causal mapping of human brain function. *Nat. Rev. Neurosci.***23**, 361–375 (2022).
17. Ganos, C. *et al.* A neural network for tics: insights from causal brain lesions and deep brain stimulation. *Brain***145**, 4385–4397 (2022).
18. Joutsa, J. *et al.* Identifying therapeutic targets from spontaneous beneficial brain lesions. *Ann. Neurol.***84**, 153–157 (2018).
19. Joutsa, J. *et al.* Brain lesions disrupting addiction map to a common human brain circuit. *Nat. Med.***28**, 1249–1255 (2022).

20. Reich, M. M. *et al.* A brain network for deep brain stimulation induced cognitive decline in Parkinson's disease. *Brain***145**, 1410–1421 (2022).
21. Schaper, F. L. W. V. J. *et al.* Mapping Lesion-Related Epilepsy to a Human Brain Network. *JAMA Neurol.***80**, 891 (2023).
22. Corbetta, M. *et al.* Common Behavioral Clusters and Subcortical Anatomy in Stroke. *Neuron* **85**, 927–941 (2015).
23. Koenigs, M. *et al.* Focal brain damage protects against post-traumatic stress disorder in combat veterans. *Nat. Neurosci.***11**, 232–237 (2008).
24. Raymont, V., Salazar, A., Krueger, F. & Grafman, J. "Studying Injured Minds" – The Vietnam Head Injury Study and 40 Years of Brain Injury Research. *Front. Neurol.***2**, (2011).
25. Boes, A. D. *et al.* Network localization of neurological symptoms from focal brain lesions. *Brain J. Neurol.***138**, 3061–3075 (2015).
26. Fox, M. D. Mapping Symptoms to Brain Networks with the Human Connectome. *N. Engl. J. Med.***379**, 2237–2245 (2018).
27. Yeo, B. T. *et al.* The organization of the human cerebral cortex estimated by intrinsic functional connectivity. *J. Neurophysiol.***106**, 1125–1165 (2011).
28. Murtagh, F. & Legendre, P. Ward's Hierarchical Agglomerative Clustering Method: Which Algorithms Implement Ward's Criterion? *J. Classif.***31**, 274–295 (2014).
29. Peel, L., Larremore, D. B. & Clauset, A. The ground truth about metadata and community detection in networks. *Sci. Adv.***3**, e1602548 (2017).
30. Winkler, A. M., Ridgway, G. R., Webster, M. A., Smith, S. M. & Nichols, T. E. Permutation inference for the general linear model. *NeuroImage***92**, 381–397 (2014).
31. Maller, J. J. *et al.* Revealing the Hippocampal Connectome through Super-Resolution 1150- Direction Diffusion MRI. *Sci. Rep.***9**, 2418 (2019).
32. Pauli, W. M., Nili, A. N. & Tyszka, J. M. A high-resolution probabilistic in vivo atlas of human subcortical brain nuclei. *Sci. Data***5**, 180063 (2018).
33. Schaefer, A. *et al.* Local-Global Parcellation of the Human Cerebral Cortex from Intrinsic Functional Connectivity MRI. *Cereb. Cortex***28**, 3095–3114 (2018).
34. Freeman, R., Baron, R., Bouhassira, D., Cabrera, J. & Emir, B. Sensory profiles of patients with neuropathic pain based on the neuropathic pain symptoms and signs. *PAIN***155**, 367– 376 (2014).
35. Hermens, D. F. *et al.* Neuropsychological Clustering Highlights Cognitive Differences In Young People Presenting With Depressive Symptoms. *J. Int. Neuropsychol. Soc.***17**, 267– 276 (2011).
36. Kelly, D. L. *et al.* Biological Basis for the Clustering of Symptoms. *Semin. Oncol. Nurs.***32**, 351–360 (2016).
37. Burgdorf, J. & Panksepp, J. The neurobiology of positive emotions. *Neurosci. Biobehav. Rev.***30**, 173–187 (2006).

38. Cheramy, A., Leviel, V. & Glowinski, J. Dendritic release of dopamine in the substantia nigra. *Nature***289**, 537–543 (1981).
39. Haber, S. N. & Fudge, J. L. The Primate Substantia Nigra and VTA: Integrative Circuitry and Function. *Crit. Rev. Neurobiol.***11**, (1997).
40. Schott, B. H. *et al.* Mesolimbic Functional Magnetic Resonance Imaging Activations during Reward Anticipation Correlate with Reward-Related Ventral Striatal Dopamine Release. *J. Neurosci.***28**, 14311–14319 (2008).
41. Wise, R. A. Roles for nigrosriatal—not just mesocorticolimbic—dopamine in reward and addiction. *Trends Neurosci.***32**, 517–524 (2009).
42. Mantani, T., Okamoto, Y., Shirao, N., Okada, G. & Yamawaki, S. Reduced activation of posterior cingulate cortex during imagery in subjects with high degrees of alexithymia: A functional magnetic resonance imaging study. *Biol. Psychiatry***57**, 982–990 (2005).
43. Dedovic, K. & Ngiam, J. The cortisol awakening response and major depression: examining the evidence. *Neuropsychiatr. Dis. Treat.* 1181 (2015) doi:10.2147/NDT.S62289.
44. Hall, B. S., Moda, R. N. & Liston, C. Glucocorticoid mechanisms of functional connectivity changes in stress-related neuropsychiatric disorders. *Neurobiol. Stress***1**, 174–183 (2015).
45. Juruena, M. F., Bocharova, M., Agustini, B. & Young, A. H. Atypical depression and nonatypical depression: Is HPA axis function a biomarker? A systematic review. *J. Affect. Disord.***233**, 45–67 (2018).
46. Lamers, F. *et al.* Evidence for a differential role of HPA-axis function, inflammation and metabolic syndrome in melancholic versus atypical depression. *Mol. Psychiatry***18**, 692–699 (2013).
47. Riva-Posse, P. *et al.* Defining Critical White Matter Pathways Mediating Successful Subcallosal Cingulate Deep Brain Stimulation for Treatment-Resistant Depression. *Biol. Psychiatry***76**, 963–969 (2014).
48. Riva-Posse, P. *et al.* A connectomic approach for subcallosal cingulate deep brain stimulation surgery: prospective targeting in treatment-resistant depression. *Mol. Psychiatry***23**, 843–849 (2018).
49. Ying, X. An Overview of Overfitting and its Solutions. *J. Phys. Conf. Ser.***1168**, 022022 (2019).
50. Ruspini, E. H. A new approach to clustering. *Inf. Control***15**, 22–32 (1969).

Methods

Complete methodological details can be found in the online supplement.

Description of Datasets

Primary Dataset

Primary analyses were performed using data from Phases II and III of VHIS.[1,2] In this study, 196 Vietnam Veterans with various stable, penetrating brain lesions were assessed at multiple time points over a 45-

year period. Veterans completed various self-report and observational inventories containing information on multiple distinct neuropsychiatric symptoms, diagnoses, traits, and behaviors, including the Beck Depression Inventory (BDI-II[3]),

Minnesota Multiphasic Personality Inventory (MMPI[4]), Clinician-Administered PTSD Scale for

DSM-IV (CAPS-IV[5]), adaptation of the Marilyn Albert remote memory battery[6],

Neurobehavioral Rating Scale (NBR[7]), Bear-Fedio Inventory[8], Profile of Mood States (POMS[9]), and the Structured Clinical Interview for the DSM-IV (SCID[10]).

We included all participants that completed a head CT scan and at least one complete behavioral inventory. We removed all items that had 1 or less responses. Altogether, this yielded 196 participants and 185 items (Table S1). We ensured that for each measure, a higher score indicated more of the associated behavior (e.g., a higher score on BDI sadness item means higher levels of sadness). We then rank transformed all scores to be on the same scale.

Validation Datasets

Our validation analyses used 10 independent, previously published datasets[11–13] which measured depression scores before and after TMS (studies=5) or DBS (studies=5). Each dataset also recorded each patient's stimulation site. In nine of these datasets (n=252) patients were stimulated at varying locations. Seven of these studies targeted MDD improvement (4 TMS, 3 DBS), and two DBS studies targeted Parkinson's and epilepsy improvement, all across varying treatment sites. The connectivity of patients' treatment sites in these datasets were computed using the normative connectome. TMS depression patients in the tenth dataset (n=302) were all treated for MDD and stimulated in the same location in the dlPFC using a coordinate from the MNI brain atlas. However, since all patients in this dataset completed a baseline resting-state fMRI scan, we were able to compute the connectivity of patients' treatment sites on an individual basis.

For all datasets, only patients with pre- and post-treatment depression scores as well as their stimulation site were included. See Table S7 for full dataset characteristics. All depression scores were rank transformed to be on the same scale and to match the original analyses. Each DBS site was inverted due to anti-correlation with TMS sites. Patients in both the primary and validation datasets provided informed consent to the original data collection or retrospective analysis was approved by the institutional review board and/or equivalent ethical committees.

The stimulation sites of Datasets 1-9 were localized as described in Siddiqi et al. (2021)[11], whereas stimulations sites of Dataset 10 were localized as a decaying sphere with maximum radius 12mm as described in Fox et al. (2013)[14]. Due to the collection of individualized connectivity in Dataset 10, imaging parameters and processing varied from the datasets using the normative connectome. The resting-state fMRI was processed using CONN (RRID:SCR_009550)[15] including motion realignment, atlas

registration, ART based outlier detection, bandpass filtering .008-.09 Hz, and white matter, ventricular, and grey matter signal regression. See Elbau et al. (2023)[12] for imaging parameters.

Statistical Analysis

All statistical analyses were conducted using MATLAB R2023a and visualizations were made using Gephi 0.10, Surf Ice 13.0.1, and python 3.9.13 unless otherwise specified.

Mapping Circuits to Behaviors

We used lesion network mapping, a previously validated method, to create whole brain “circuit maps” of each individual symptom or behavior in our VHIS dataset.[16,17] For each participant, we computed a whole-brain normative connectivity profile, indicating the connectivity of their lesion location to every voxel in the brain (228,453 voxels). Connectivity was estimated based on a large normative connectome of 1000 healthy patients’ resting state functional connectivity data.[18] A circuit map for each of the 185 items was then created by calculating the Pearson’s correlation between these lesion connectivity profiles and the item score for each brain voxel (Fig. 1).

Clustering

We clustered the individual circuit maps following previously published methods.[19] First, we quantified the strength of the 185 behavioral circuit maps’ relationship to one another by computing the spatial correlation between each pair of maps. To ensure the differences between the behavioral maps’ correlation profiles were not a consequence of randomness, we calculated whether the average standard deviation of the resulting cross-correlation matrix was stronger than chance (Fig 2a-b). The cross-correlation matrix was then clustered using Ward’s hierarchical clustering algorithm (Fig. 2c).[20] The strength of the clustering was measured using the silhouette coefficient, a metric of within-cluster similarity and between-cluster difference.[21] We chose an optimal number of clusters based on the clustering solution that maximized the silhouette coefficient.

To test for significance, we used permutation testing as previously described.[11,19] Permutation testing involved creating a null model by randomly assigning each participant’s lesion to another participant’s behavioral scores. After conducting 25,000 iterations, we computed a p-value equal to the percentage of cases in which the permuted silhouette value was greater than the real value. We hypothesized that the optimal number of clusters would have a stronger silhouette value than expected by chance.

Control Analyses

After the optimal number of clusters was identified, we ran various control analyses to confirm our results and ensure that they were not driven by other factors. To see if the lesion data added important information to the results or if the results were driven primarily by the behavioral data, we re-computed all the primary analyses using only the original behavioral data (Fig. 2d). We then compared the behavioral-

only results to the behavioral-anatomical results. We also used other community detection methods to confirm our findings in order to account for clustering algorithm biases, per standards of best practice[22,23] (Text S1, Figure S1). To confirm that our results were not driven by a particular choice in data transforms or thresholds, we repeated our analyses with various methodological variations including data transformations, thresholding, and accounting for missing data (Text S2, Table S2).

Examining Properties of Clusters

We then used a leave-one-out analysis to explore which behaviors were most influential in each cluster and to ensure that none of those individual behaviors were driving the results. The leave-one-out analysis was completed by systematically removing an individual behavioral circuit map from its cluster and averaging the remaining behavioral maps. The modified cluster map and the individual behavioral map were then compared using a spatial correlation. This was repeated across all clusters and behaviors (Tables S3-5).

The behaviors with the strongest leave-one-out values indicate the most central behaviors in each cluster (Figure S2). We then used a one-sample t-test to determine whether these leave-one-out spatial correlations were significantly stronger than zero, in order to determine that no single behavior was driving the results.

Deriving Final Behavior Cluster Maps

Before deriving our final cluster maps, we removed any behavioral circuit maps that resulted in a negative spatial correlation from our leave-one-out analysis to account for outliers in each cluster. Finally, we averaged all of the individual behavior circuit maps within each individual cluster (Fig. 3). The resulting cluster maps indicate the connectivity of lesions that modify each respective cluster.

We quantified the strength of each cluster map based on the absolute mean and absolute peak voxel values. We then used permutation testing (25,000 permutations) to determine whether the absolute mean and absolute peak values were stronger than chance. Per the Westfall Young method, we then used the distribution of these absolute peak values to identify a significant threshold value ($p<.05$) for each cluster and thresholded each respective cluster map to determine all significant voxels.[24] In order to ensure the maps were not a result of small data cleaning decisions, we re-computed them using a variety of different cleaning methods (Table S6).

Predicting Clinical Outcomes

Our final set of analyses used 10 independent, previously published TMS and DBS datasets to determine the validity and potential clinical utility of the clusters. These analyses investigated whether treatment site connectivity to each independent cluster network could predict clinical antidepressant outcomes after neuromodulation treatments.

The first step in this analysis was deriving patient-specific treatment site connectivity profile. In nine of our datasets, this was accomplished by computing the whole brain connectivity of each participant's treatment location using a large normative connectome (n = 1,000), similar to lesion network mapping. In our tenth dataset, this was accomplished by computing the whole brain connectivity of each participant's treatment location using their individual resting-state fMRI. We then calculated the connectivity of each site to each cluster using Pearson's correlation (Fig. 4). Finally, we used these values to predict the difference in antidepressant response using a partial correlation which accounted for both baseline depression scores and the other cluster's connectivity values. To account for dataset, each of the 10 datasets was analyzed individually and combined into a weighted mean.

Methods References

1. Koenigs, M. *et al.* Focal brain damage protects against post-traumatic stress disorder in combat veterans. *Nat. Neurosci.***11**, 232–237 (2008).
2. Raymont, V., Salazar, A., Krueger, F. & Grafman, J. "Studying Injured Minds" – The
3. Vietnam Head Injury Study and 40 Years of Brain Injury Research. *Front. Neurol.***2**, (2011).
4. Beck, A. T., Steer, R. A. & Brown, G. K. Manual for the beck depression inventory-II. *San Antonio TX Psychol. Corp.***1**, 10.1037 (1996).
5. Hathaway, S. R. & Mckinley, J. C. A Multiphasic Personality Schedule (Minnesota) : I. Construction of the Schedule. *J. Psychol.***10**, 249–254 (1940).
6. Blake, D. D. *et al.* The development of a Clinician-Administered PTSD Scale. *J. Trauma. Stress***8**, 75–90 (1995).
7. Ferguson, M. A. *et al.* A human memory circuit derived from brain lesions causing amnesia. *Nat. Commun.***10**, 3497 (2019).
8. Levin, H. S. *et al.* The neurobehavioural rating scale: assessment of the behavioural sequelae of head injury by the clinician. *J. Neurol. Neurosurg. Psychiatry***50**, 183–193 (1987).
9. Bear, D. M. & Fedio, P. Quantitative Analysis of Interictal Behavior in Temporal Lobe Epilepsy. *Arch. Neurol.***34**, 454–467 (1977).
10. McNair, D. M., Droppleman, L. F. & Lorr, M. *Profile of Mood States (POMS)*. (Educational and Industrial Testing Service, 1971). First, M. B. & Gibbon, M. The Structured Clinical Interview for DSM-IV Axis I Disorders (SCID-I) and the Structured Clinical Interview for DSM-IV Axis II Disorders (SCID-II). in *Comprehensive handbook of psychological assessment, Vol. 2: Personality assessment* 134–143 (John Wiley & Sons, Inc., 2004).
11. Siddiqi, S. H. *et al.* Brain stimulation and brain lesions converge on common causal circuits in neuropsychiatric disease. *Nat. Hum. Behav.***5**, 1707–1716 (2021).
12. Elbau, I. G. *et al.* Functional Connectivity Mapping for rTMS Target Selection in Depression. *Am. J. Psychiatry***180**, 230–240 (2023).
13. Blumberger, D. M. *et al.* Effectiveness of theta burst versus high-frequency repetitive transcranial magnetic stimulation in patients with depression (THREE-D): a randomised non-inferiority trial. *The*

*Lancet***391**, 1683–1692 (2018).

14. Fox, M. D., Liu, H. & Pascual-Leone, A. Identification of reproducible individualized targets for treatment of depression with TMS based on intrinsic connectivity. *NeuroImage***66**, 151– 160 (2013).
15. Nieto-Castanon, A. *Handbook of functional connectivity Magnetic Resonance Imaging methods in CONN*. (Hilbert Press, 2020).
16. Boes, A. D. *et al.* Network localization of neurological symptoms from focal brain lesions. *Brain J. Neurol.***138**, 3061–3075 (2015).
17. Fox, M. D. Mapping Symptoms to Brain Networks with the Human Connectome. *N. Engl. J. Med.***379**, 2237–2245 (2018).
18. Yeo, B. T. *et al.* The organization of the human cerebral cortex estimated by intrinsic functional connectivity. *J. Neurophysiol.***106**, 1125–1165 (2011).
19. Siddiqi, S. H. *et al.* Distinct Symptom-Specific Treatment Targets for Circuit-Based Neuromodulation. *Am. J. Psychiatry* (2020) doi:10.1176/appi.ajp.2019.19090915.
20. Murtagh, F. & Legendre, P. Ward's Hierarchical Agglomerative Clustering Method: Which Algorithms Implement Ward's Criterion? *J. Classif.***31**, 274–295 (2014).
21. Rousseeuw, P. J. Silhouettes: A graphical aid to the interpretation and validation of cluster analysis. *J. Comput. Appl. Math.***20**, 53–65 (1987).
22. Peel, L., Larremore, D. B. & Clauset, A. The ground truth about metadata and community detection in networks. *Sci. Adv.***3**, e1602548 (2017).
23. Kettenring, J. R. The Practice of Cluster Analysis. *J. Classif.***23**, 3–30 (2006).
24. Winkler, A. M., Ridgway, G. R., Webster, M. A., Smith, S. M. & Nichols, T. E. Permutation inference for the general linear model. *NeuroImage***92**, 381–397 (2014).

Figures

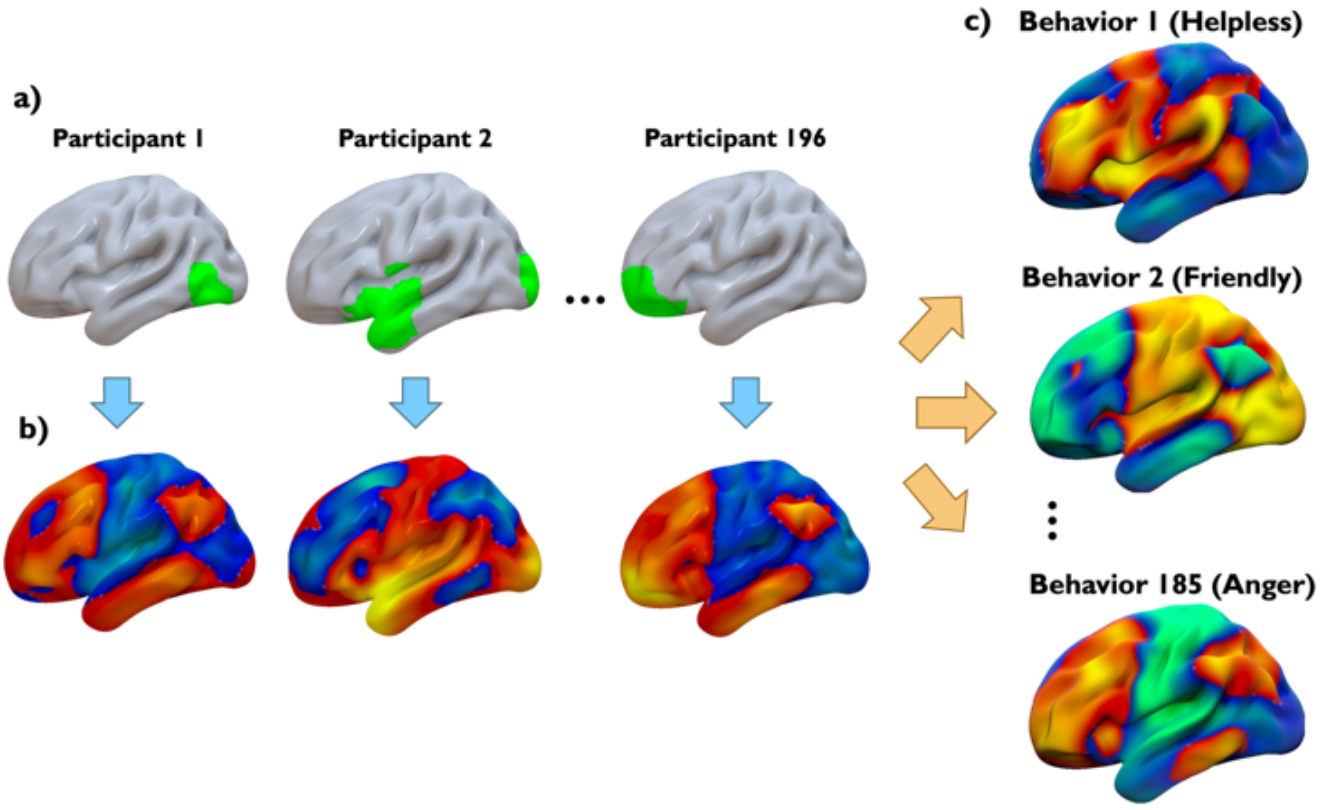

Figure 1

Mapping Circuits to Behaviors

We created 185 circuit maps representing each measured behavior. **a)** 196 lesions were localized and mapped to a standard MNI 152 brain atlas. **b)** We computed the connectivity of each participant's lesion to every brain voxel using a normative connectome database (N=1,000). **c)** We identified the brain circuit connected to lesions which are associated with an increase or decrease in each of the 185 behaviors.

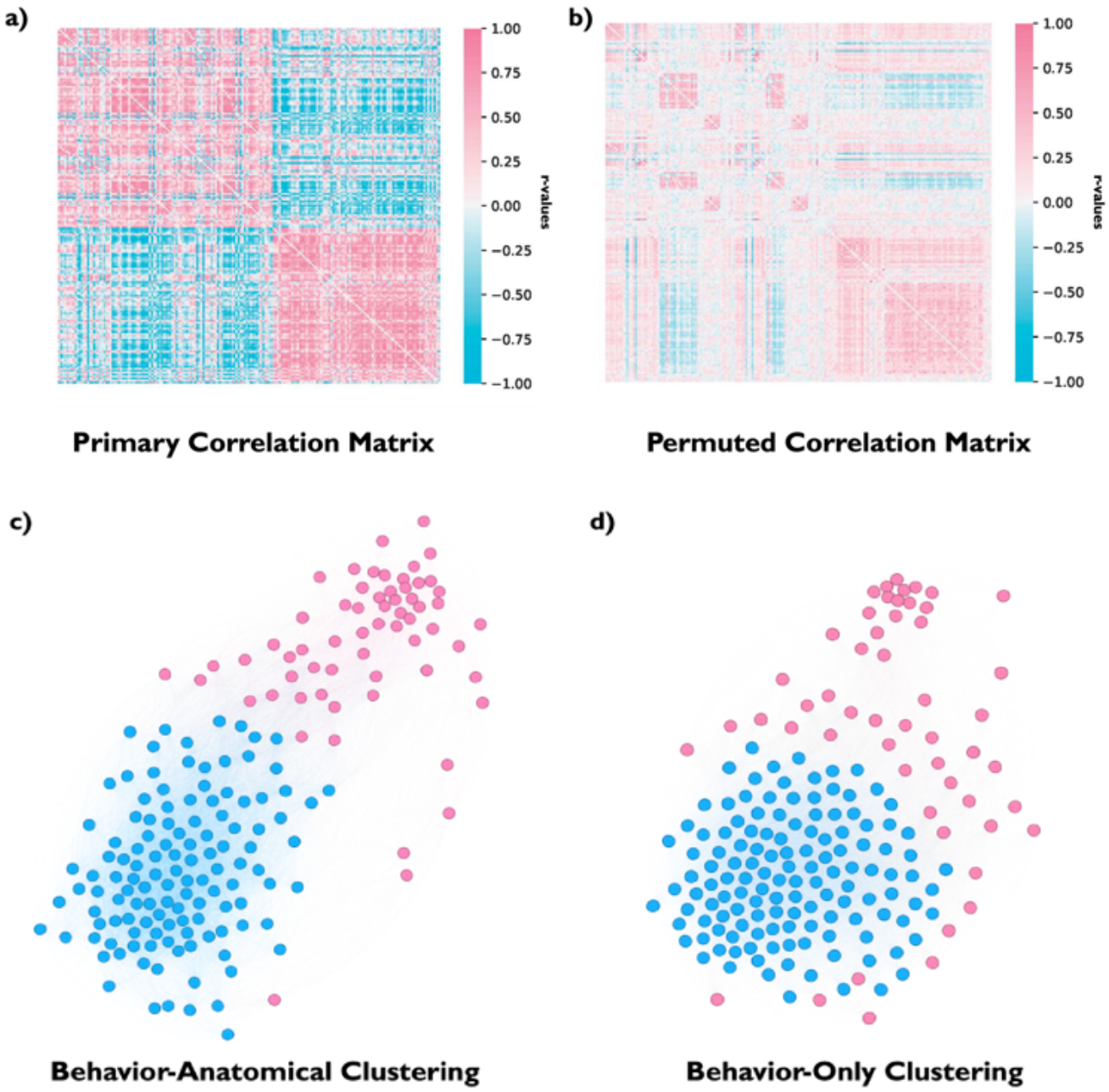

Figure 2

Clustering of Behavioral Circuits.

185 behavioral circuit maps fell into two overall clusters. **a)** Most of the behavioral circuit maps showed strong positive or negative correlation with the remaining circuit maps, suggesting the presence of two overall clusters. **b)** Randomly permuted correlation matrices did not show clear positive-negative dissociation, with significantly weaker variance than the real data (p=0.025). **c)** Force-directed graph visualization depicting the two overall clusters. See Fig. 3 for the mean anatomical renderings of each cluster. **d)**Similar clustering was not evident when using behavioral metrics alone, in the absence of anatomical data.

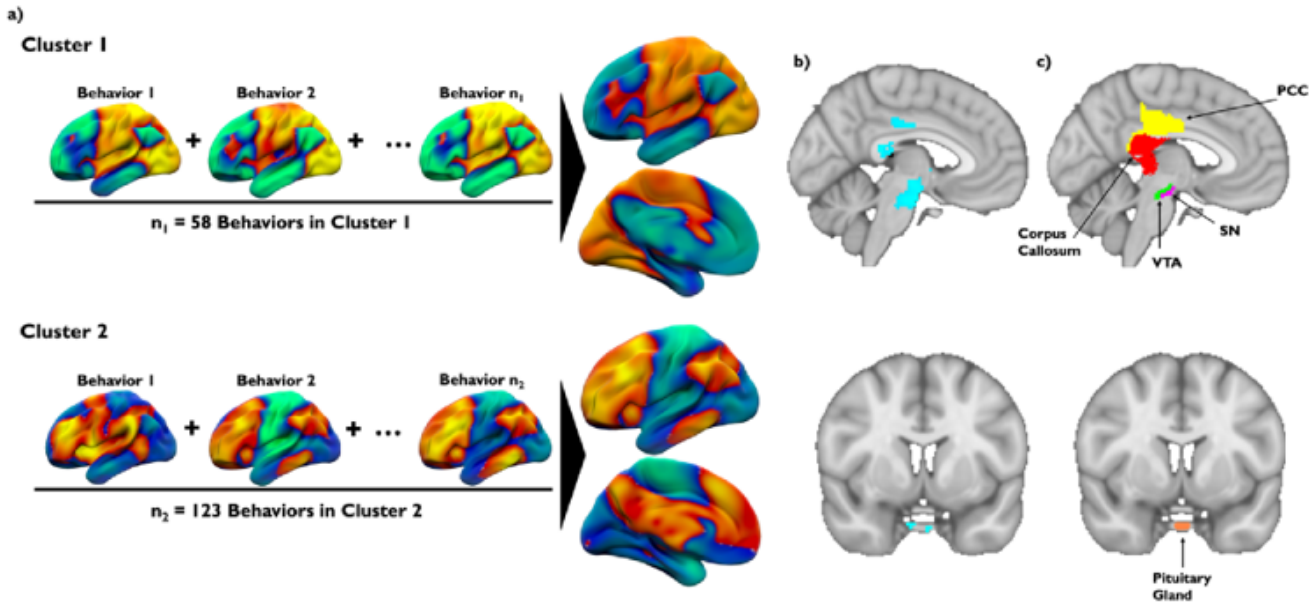

Figure 3

Deriving Final Behavior Cluster Maps & Peaks

We created an average circuit map for each respective cluster and identified the significant peaks in each map. **a)** To compute the average cluster circuit maps for positive and negative affect, we averaged the behaviors in each cluster and then calculated the correlation between the mean behavioral score and lesion connectivity to each brain voxel. This resulted in two distinct maps representing the circuits connected to lesions that modify each behavioral cluster respectively. **b-c**) The absolute peak of each cluster was stronger than expected by chance (25,000 permutations). We used the Westfall-Young method to determine the most relevant peaks ($p<.05$). Peaks in Cluster 1 are in the PCC, VTA, SN, and corpus callosum connected to the cingulate gyrus.[31–33] Peaks in Cluster 2 are in the pituitary gland.

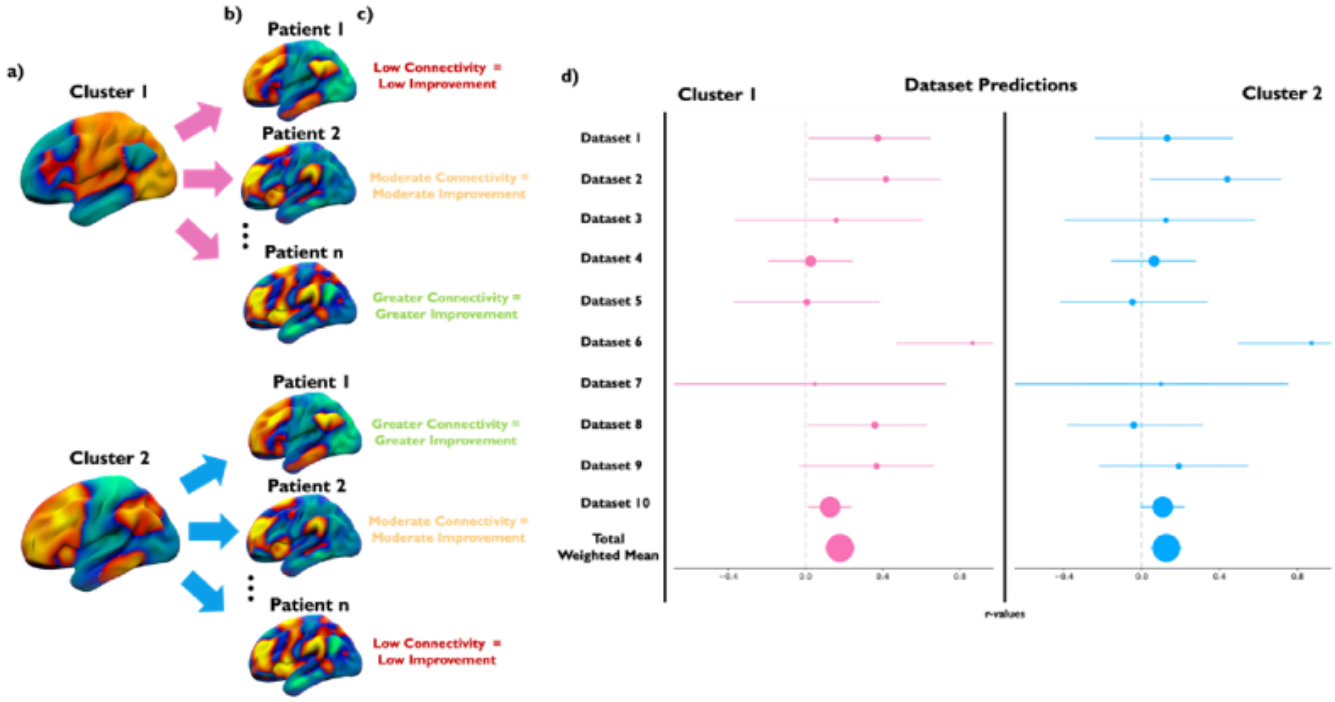

Figure 4

Predicting Clinical TMS & DBS Antidepressant Outcomes

We showed that treatment site connectivity to each of our clusters independently predicted antidepressant outcomes. **a-c)** In every dataset, we calculated the connectivity of Cluster 1 and Cluster 2 to every patient's stimulation site. DBS sites were inverted due to anti-correlation with TMS sites. We then used this cluster connectedness to predict antidepressant treatment outcomes. **d)** This process was repeated for every dataset and then combined using a weighted mean to account for dataset size. Relative sample size is depicted by size of the circle and 95% confident interval depicted by corresponding lines.

Supplementary Files

This is a list of supplementary files associated with this preprint. Click to download.

- Frandsenetaldualclustersup231212.docx